SYNTHESIS OF MONODISPERSE SILICA MICROPARTICLES WITH TUNABLE SHAPE AT FLUID INTERFACES

Aiping Fang[1], **Cédric Gaillard**[2]
[1]*Nano, BIA, UR 1268, INRA, rue de la Géraudière, 44316 Nantes, France*
[2]*ISD & BIBS Microscopie, BIA, UR 1268, INRA, rue de la Géraudière, 44316 Nantes, France*

ABSTRACT

We have previously presented the synthesis of monodisperse doughnut-shaped silica microparticles by a simple droplet-based microfluidic approach. [1] Here we further studied their formation mechanism triggered by rapid solvent diffusion and the parameters for shape control. Interestingly, it is found that the shape of the silica particles can be tuned by the ratio of droplet diameter to microfluidic channel height (D_0/h) and the local Peclet number, P_e. We demonstrate the monodisperse silica microparticles with tunable shape at fluid interfaces in microfluidics. By varying the channel aspect ratio (R_{asp}) and P_e, we have achieved silica particles with variable shapes of sphere, dimpled sphere, bowl, doughnut.

KEYWORDS

Droplet-based microfluidics, silica, tunable shape, fluid interface.

INTRODUCTION

Silica particles have demonstrated potentials in numerous fields such as separation science, drug delivery, or catalysis. [2] However, their polydispersity, either in size or shape, presents a major challenge in understanding and controlling the mass-transport properties, which in turn introduces a striking lack, for example, in understanding the effect of particle size and shape in the fields of drug delivery and material science. Recently, there has been a great attention to the synthesis of anisotropic silica particles. On the other hand, microfluidics provides a straightforward and robust approach to obtain highly monodisperse droplets, one at a time and with an incomparable degree of control over size. In addition, the characteristic parabolic velocity profile in microfluidic channel introduces new phenomena in hydrodynamics. Therefore, we applied on chip emulsification and solvent diffusion to synthesize silica particles with controlled size and shape. Silica shape can be tuned by D_0/h and P_e varying from sphere, dimpled sphere to bowl and doughnut. The interesting results would help to promote the potential applications of silica materials in separation, adsorption, catalysis and drug delivery, [3-4] especially in the case that particle shape has a strong impact on their performance. [5]

EXPERIMENT

Droplets were achieved on chip using a flow focusing device (Fig. 1). The microfluidic channels were obtained by irreversible thermal bonding of a PDMS replica onto a flat PDMS slab and the resulting chip was used directly without any surface modification. The continuous oil phase, dimethyl carbonate (DMC, 99 %, Sigma-Aldrich), was supplied to the device through inlet 1 using a digitally controlled syringe pump (Harvard Apparatus PHD 2000, USA). The dispersed aqueous phase was supplied through inlet 2 in the same manner. The silica sol precursor solution was used as aqueous phase, which was prepared by mixing 1.0 mL of tetraethyl orthosilicate (TEOS, 99.0 %, Fluka), 0.1 mL of triethyl amine (TEA, 99.5 %, Fluka) with 5.0 mL of water (MilliQ, 18 MΩ.cm). This mixture was stirred at room temperature until one single homogeneous phase appeared (~ 5 hours).

The respective flow rates were 3.00 and 0.05 mL/hr. After the breakup junction, the emulsion droplets travelled along a channel with its width fixed at 200 µm and its height varying in the range of 60-240 µm, indicative of a R_{asp} of 0.3 to 1.2. Its total diffusion length, l, was either 36, 84, 109 or 137 cm, depending on the drying time required. Particles were collected from outlet 3.

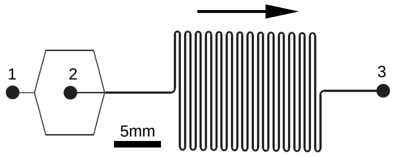

Figure 1: Scheme of the PDMS device used for this work.

Droplets and particles were observed in situ using an Olympus IX51 inverse microscope (Olympus) coupled with a digital camera (Sony, SCD-SX90). Scanning electron microscope (SEM) images were obtained with JEOL 7600F instrument. To better understand their morphology, silica particles were cured in epoxy resin and sectioned into ultrathin slices for tunnelling electron microscope (TEM) observations.

P_e is defined as the ratio of two characteristic times in the drying process: [6] time required for a sol nanocluster (SN) to diffuse from the edge of the droplet to its center, R^2/D_{dif}. Here R and D_{dif} are the radius of the droplet ($R = 1/2\ D_0$, Fig. 2) and the SN diffusion coefficient, respectively, while the other is the time required for a droplet to dry, τ_d. D_{dif} is calculated by Stokes-Einstein equation [6] with the SN's size of 25 nm. [1] Thus, $P_e = R^2/\ \tau_d\ D_{dif}$.

As previously stated, uniform W/O droplets were generated with the flow focusing PDMS devices and subsequently underwent in situ rapid solvent diffusion in microfluidic channel. After their generation, the sol droplets were found subject to consecutive stages of shrinkage, deformation, buckling, condensation and solidification. [1] The resulting silica particle shape, however, strongly depended on the R_{asp}. Besides doughnut-like shape, we also reproducibly achieved bowl-like shape. Fig. 2 compares the real-time droplet transformations in the microfluidic channels at two different R_{asp} and their resulting morphology characterized by SEM and TEM. From Fig. 2Ac, it is evident that, when $R_{asp} = 0.4$, droplets tend to deform symmetrically in the cross flow direction after shrinkage, resulting in lateral buckling toward a final doughnut shape (Fig. 2A d-f); On the contrary, when $R_{asp} = 1.1$, deformation can occur at any point of the droplet free surface (Fig. 2Bc), leading to asymmetric buckling and eventually to bowl-like silica particles (Fig. 2B d-f). The cross sectional view of the particles by TEM in Fig. 2h clearly demonstrates their different morphologies simply through varying the R_{asp}.

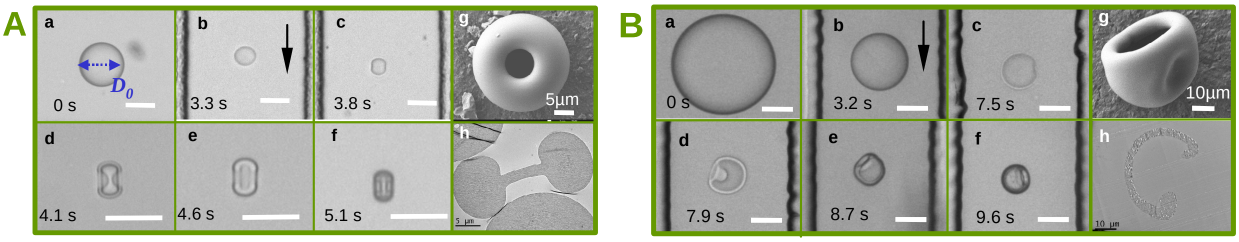

Figure 2: Real-time droplet shape transformation at fluid interfaces at P_e much greater than unity when forming A) doughnut-shaped ($P_e = 52$, $R_{asp} = 0.4$, $D_0/h = 0.92$) or B) bowl-shaped ($P_e = 45$, $R_{asp} = 1.1$, $D_0/h = 0.57$) silica particles: (a) droplet generation; (b) shrinkage; (c) deformation; (d) buckling; (e) condensation; and (f) solidification; (g) SEM and (h) TEM images of the as-formed particles. The time indicates the actual time from the droplet generation. The arrows depict the flow direction in channels. The dark edges in images correspond to the side wall of serpentine channel with a total length of 36 cm. Scale bar is 50 µm unless otherwise stated.

It has to be mentioned that the above two shapes are constantly achieved when $P_e >> 1$. It is found that R_{asp} plays a dominant role in particle shape when P_e is much greater than unity. Doughnut-shape and bowl-shape were constantly obtained when $D_0/h > 0.8$ and $D_0/h < 0.8$, respectively (Fig. 2).

While we are able to demonstrate that D_0/h plays a dominant role in silica particle shapes when $P_e >> 1$ in fluid interfaces in microfluidic channels, one may wonder the scenarios when P_e is reduced close to unity. According to the equation $P_e = R^2/ \tau_d D_{dif}$., reducing P_e means increasing droplet drying time in microfluidic channel or/and decreasing diffusion time of SNs. In our case, we used a high water content both in continuous phase and in emulsion droplets for slow water diffusion from the droplets. Thus, we used DMC with high water content as the continuous phase, and highly diluted precursor solutions (typically 10-time dilution) as water disperse phase. In addition, the drying serpentine channels were prolonged up to 137 cm for sufficient drying. In Fig. 3, silica particles with various shapes are displayed through tuning both the parameter D_0/h and P_e. When P_e is small enough ($P_e < 10$) , surprisingly the silica particle shape is independent of D_0/h and are found spherical (Fig. 3a & 3d). When P_e is increased to a medium value around 10, dimpled spheres are observed. However, in the case of $D_0/h < 0.8$, single-dimpled spheres are achieved (Fig. 3b) instead of double-dimpled spheres in the case of $D_0/h > 0.8$ (Fig. 3e). The results imply that, a small P_e generally favors spherical shape, independent of the D_0/h. When $P_e > 10$, the parameter D_0/h starts to play a dominant role, yielding two dominant shapes with a threshold at 0.8: bowl-like and doughnut-like shape for $D_0/h < 0.8$ and $D_0/h > 0.8$, respectively.

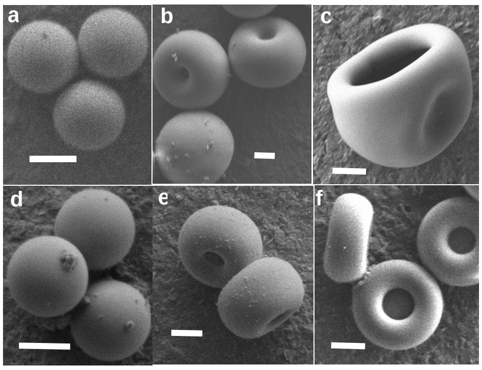

Figure 3: Tuning the shape of silica particles by varying P_e and D_0/h: a) $P_e = 4.1$, $D_0/h = 0.32$; b) $P_e = 12$, $D_0/h = 0.62$; c) $P_e = 45$, $D_0/h = 0.57$; d) $P_e = 6.5$, $D_0/h = 0.97$; e) $P_e = 10$, $D_0/h = 0.80$; f) $P_e = 52$; $D_0/h = 0.92$. It is found that small P_e favors spherical shape and high D_0/h favors disk shape. In order to achieve small P_e, diluted precursor solutions and prolonged microfluidic channels (l= 36~137 cm) were used. Scale bar: 10 µm.

Coupled with hydrodynamics and mechanical instabilities at fluid interface, the non-uniform solvent diffusion at the periphery of the confined droplets is responsible for the tunable shape. [7] The characteristic parabolic velocity profile in microfluidic channels renders droplet-based microfluidics a unique method to prepare silica particles with morphology control. The velocity distribution at a cross section will be parabolic in shape with the maximum velocity at the center, essentially zero in contact with the wall. As a result, water within an emulsion droplet is removed at different rate across the circumferential region of droplets. Droplet's circumferential region on xz plane (channel cross section view as showed in Fig. 4) is subject to different rate when it translates downstream with an entourage of the continuous phase. This difference becomes significant as soon as either the channel aspect ratio or the confinement becomes large. In the fast drying regime ($P_e >> 1$) when $D_0/h > 0.8$, the significant confinement renders solvent diffusion minimum at the top and bottom of droplet surface, maximum at the lateral direction (right in Fig. 4A), yielding the first formation of viscoelastic shell at the lateral direction. This is confirmed by the lateral deformation of droplet in forming doughnut-like shape in Fig. 2Ac. On the contrary, confinement is not significant in the case of $D_0/h < 0.8$. Water diffusion is uniform in all radial positions (left in Fig. 4A). The droplets tend to shrink isotropically and viscoelastic shell forms in any energy well at the free surface of droplet (Fig. 2Bc). Further drying and buckling result in bowl-like shape as observed in Fig. 2B d-f.

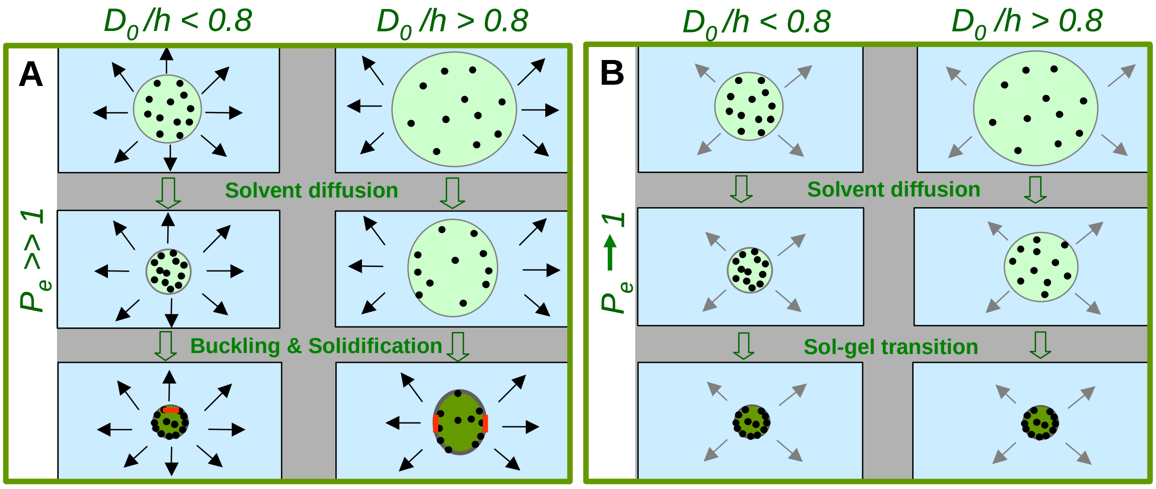

Figure 4: Schematics of the non-uniform solvent diffusion introducing A) non-symmetric and symmetric buckling instability (indicated by red color) for a $D_0/h < 0.8$ and $D_0/h > 0.8$, respectively; and B) slow diffusion at $P_e < 10$, where buckling is absent. Black and grey arrows show fast and slow water diffusion; respectively.

In the slow drying regime when $P_e < 10$, the global internal mass transfer is much faster compared to the hindered water transfer at fluid interface, resulting in homogenous SNs across the droplet. As seen from Fig. 4B, the droplets don't buckle but shrink isotropically, and undergo sol-gel transition to form spherical dense particles.

We introduce a one-step approach for the synthesis of monodisperse silica particles with shape control : loss of the water contained in the sol triggers both the gel transition and the shape transformation of the initially spherical droplets at fluid interfaces. This interfacial evaporation driven shape transformation has already been observed in spray-drying.[8] To the best of our knowledge, this is the first trial for accurate engineering of anisotropy in silica particles by a microfluidic approach. This method is completely general and it allows in situ encapsulation of functional molecules for drug delivery carrier. In order to control the morphology, one would just need to tune parameters such as the sol concentration, sol droplet size, channel dimensions.

REFERENCES

[1] A. Fang, C. Gosse, C. Gaillard, J.-P. Douliez, *Proceedings of MicroTAS 2011*, pp. 15-17, (2011).
[2] H. T. Fan, J. Li, Z. C. Li, T. Sun, *Appl. Surf. Sci.* **2012**, *258*, 3815.
[3] J. Nakazawa, B. J. Smith, T. Stack, P. Daniel, *J. Am. Chem. Soc.* **2012**, *134*, 2750.
[4] a) J. F. Chen, H. M. Ding, J. X. Wang, L. Shao, *Biomaterials* **2004**, *25*, 723. b) I. I. Slowing, J. L. Vivero-Escoto, C. W. Wu, V. S. Lin, *Adv. Drug. Delivery Rew.* **2008**, *60*, 1278.
[5] a) J. A. Champion, Y. K. Katare, S. J. Mitragotri, *Control. Release* **2007**, *121*, 3. b) L. Tao, W. Hu, Y. Liu, G. Huang, B. D. Sumer, J. Gao, *Exp. Bio. Med.* **2011**, *236*, 20.
[6] N. Tsapis, D. Bennett, B. Jackson, D. A. Weitz, D. A. Edwards, *Proc. Natl. Acad. Sci. U.S.A.* **2002**, *99*, 12001.
[7] a) L. Pauchard, Y. Couder, *Europhys. Lett.* **2004**, *66*, 667; b) A. Fang, C. Gaillard, J.-P. Douliez, *Chem. Mater.* **2011**, *23*, 4660.
[8] a) R. Vehring, W. R. Foss, D. Lechuga-Ballesteros, *Aerosol Sci*. **2007**, *38*, 728; b) J. Bahadur, D. Sen, S. Mazumder, S. Bhattacharya, H. Frielinghaus, G. Goerigk, *Langmuir* **2011**, *27*, 8404; c) W. Liu, W. D. Wu, C. Selomulya, X. D. Chen, *Langmuir* **2011**, *27*, 12910; d) A. B. D. Nandiuanto, K. Okuyama, *Adv. Powder Tech*. **2011**, *22*, 1; e) J. Bahadur, D. Sen, S. Mazumder, B. Paul, H. Bhatt, S. G. Singh, *Langmuir*, **2012**, *28*, 1914.

CONTACT

Aiping Fang, Tel: +33- 2 40 67 51 44 or aiping.fang@nantes.inra.fr